nature communications

Article

https://doi.org/10.1038/s41467-024-51536-x

Tislelizumab plus cetuximab and irinotecan in refractory microsatellite stable and RAS wild-type metastatic colorectal cancer: a single-arm phase 2 study

Received: 9 March 2024

Accepted: 12 August 2024

Published online: 23 August 2024

Check for updates

Xiaojing Xu[1,2,5], Luoyan Ai[1,2,5], Keshu Hu[1,2,5], Li Liang[1,2,5], Minzhi Lv[2,5], Yan Wang[1,2], Yuehong Cui[1,2], Wei Li[1,2], Qian Li[1,2], Shan Yu[1,2], Yi Feng[1,2], Qing Liu[1,2], Ying Yang[3], Jiao Zhang[3], Fei Xu[3], Yiyi Yu[1,2] ✉ & Tianshu Liu[1,2,4] ✉

Immunotherapy confers little to no benefit in the treatment of microsatellite stable (MSS) metastatic colorectal cancer (mCRC). Mechanistic insights suggested that epidermal growth factor receptor (EGFR) antibody plus irinotecan might augment the tumor immune response in mCRC. Therefore, we conducted a proof-of-concept, single-arm, phase 2 study (ChiCTR identifier: ChiCTR2000035642) of a combination treatment regimen including tislelizumab (anti-PD-1), cetuximab (anti-EGFR) and irinotecan in 33 patients with MSS and *RAS* wild-type (WT) mCRC who were previously treated with ≥2 lines of therapy. The primary endpoint was met, with a confirmed objective response rate of 33%. As secondary endpoints, the disease control rate was 79%, and the median progression-free survival and overall survival were 7.3 and 17.4 months respectively. Among the 33 patients, 32 (97.0%) had treatment-related adverse events (AEs). Three (9.1%) reported grade ≥ 3 AEs, including rash ($n = 1$), neutropenia ($n = 2$). The post-hoc evaluation of dynamic circulating tumor DNA using next generation sequencing and the analysis of peripheral immune proteomics landscape using Olink revealed that lower variant allele frequency (VAF) at baseline, greater reduction in VAF on treatment, and a hot peripheral macroenvironment were associated with the treatment response independently. Our study showed the antitumor activity of tislelizumab, cetuximab, and irinotecan combination with a tolerable safety profile in previously treated MSS and *RAS* WT mCRC.

The combination of an anti-epidermal growth factor receptor (anti-EGFR) antibody (cetuximab or panitumumab) with chemotherapy is a standard treatment for patients with *RAS* and *BRAF* wild-type (WT) metastatic colorectal cancer (mCRC)[1,2]. Although these regimens are highly effective in the first- or second-line setting, the clinical benefit of the later-line standard therapies, such as regorafenib[3] or trifluridine/tipiracil[4], is limited with a high incidence of adverse events (AEs). Such later-line therapies reported an objective response rate (ORR) of 1% to 4% and a median progression-free survival (mPFS) of 1.9 to 3.2 months. In this context, despite the lack of high-level

[1]Department of Oncology, Zhongshan Hospital, Fudan University, 200032 Shanghai, China. [2]Cancer Center, Zhongshan Hospital, Fudan University, 200032 Shanghai, China. [3]Genecast Biotechnology Co., Ltd, 214104 Wuxi City, Jiangsu, China. [4]Center of Evidence-based medicine, Fudan University, 200032 Shanghai, China. [5]These authors contributed equally: Xiaojing Xu, Luoyan Ai, Keshu Hu, Li Liang, Minzhi Lv. ✉e-mail: yu.yiyi@zs-hospital.sh.cn; liu.tianshu@zs-hospital.sh.cn

evidence, re-treatment with previously administered drugs is often adopted in clinical practice. For instance, the results from the CRICKET study[5] demonstrated an ORR of 21% (confirmed ORR 14%) with the reintroduction of cetuximab plus irinotecan in the third-line setting. CHRONOS study[6] selected patients with 'zero mutation ctDNA triage' for panitumumab rechallenge, and showed an exceptional ORR of 30% (confirmed ORR 22%) for mCRC patients with *RAS* WT.

Immune checkpoint inhibitors (ICIs), such as anti-programmed cell death protein 1 (PD-1) or programmed cell death ligand 1 (PD-L1) monoclonal antibodies (mAbs), are established standards of care for patients with mismatch repair deficient (dMMR) or microsatellite instability-high (MSI-H) mCRC[7,8]. However, ICI monotherapy offered little to no effect for most of the proficient mismatch repair (pMMR) or microsatellite stable (MSS) subtype[9,10]. Hence, a combination strategy by adding tumor-targeting antibodies or cytotoxic agents to ICIs is a logical next step through changing the immune microenvironment. Besides the aforementioned clinical use, cetuximab has been reported to trigger the immunogenic cancer cell death and augment the CRC immunogenicity[11]. Increased levels of cytotoxic immune infiltrates, PD-L1, CXCR2, and LAG3 were observed after the effective cetuximab treatment in patients with mCRC, potentially providing opportunities to treat cetuximab-resistant CRCs with immunotherapy[12,13]. Importantly, cetuximab is an IgG1 mAb that has a strong antibody-dependent cell cytotoxicity (ADCC) and results in cross talk among the immune cells, including natural killer (NK) cells and dendritic cells[14,15]. This cross talk can prime the tumor antigen-specific cellular immunity and generate the antigen-specific T-lymphocyte responses[16,17]. In this scenario, cetuximab may have additive or synergetic effects with PD-1 blockade. This has been proved in patients with recurrent or metastatic head and neck squamous cell carcinoma, with the longest median overall survival (mOS) of 18.4 months achieved by cetuximab plus pembrolizumab[18]. The phase 2 CAVE study (avelumab plus cetuximab) has demonstrated an active clinical activity, with an mOS of 11.6 months and an mPFS of 3.6 months in pretreated MSS mCRCs[19], highlighting the scientific rationale of the combination. However, the result was not encouraging. Therefore, we considered that chemical agents may also play an important role. Preclinical studies found that SN-38, an active metabolite of irinotecan, could sensitize unresponsive tumors responding to anti-PD-1 therapy by engaging NK or $CD8^+$ T cells to infiltrate the tumor microenvironment (TME)[20,21], suggesting that ICIs combined with cetuximab and irinotecan may work synergically.

The circulating tumor DNA (ctDNA) can be used to detect tumor-specific alterations, and was highly consistent with tissues[22,23]. Moreover, ctDNA has been well documented to be correlated with response and survival time in the field of chemotherapy or targeted therapy[24–26]. Whether ctDNA monitoring could also predict the clinical benefit of these ICI-based combination therapies in MSS mCRCs is yet to be determined. Furthermore, tumor progression or regression is a consequence of the battle between tumor cells and host immunity. We believe that factors reflecting the systemic immunity could also predict the response, especially in the context of immunotherapy. Serum immune proteomics, with its high content, could be a suitable reflection of the global immunity[27–29].

In this work, we conducted a study to investigate the efficacy and safety of ICI combined with cetuximab and irinotecan (**TEC, T**islelizumab plus **E**rbitux and **C**PT-11) in MSS and *RAS/BRAF* WT mCRC in third or more lines settings. Furthermore, to identify which patients may benefit from TEC, we performed ctDNA profiling and plasma immune proteomics profiling using blood samples taken before and during treatment. Here, we show that TEC has antitumor activity with confirmed ORR of 33% and mOS of 17.4 months. Pretreatment ctDNA levels and immune-oncology proteins levels are associated with the response.

Results

Efficacy

Between February and September 2021, 36 patients were screened in this study. One patient did not meet the inclusion criteria, and 2 patients withdrew the informed consent for personal reasons before treatment. As a result, 33 patients had at least 1 cycle of treatment (Fig. 1). Among them, 22 patients (67%) failed at least 3 lines of treatment. The median time from the initial diagnosis of metastasis to enrollment was 30.2 months. The baseline characteristics are presented in Table 1 and Supplementary Table 1.

At the time of the data cutoff on December 12, 2022, the median follow-up time was 17.6 months (1.1–21.8 months). All 33 patients had at least 1 imaging assessment for efficacy. Radiographic partial response (PR) was observed in 12 patients (36%), and 14 patients (42%) achieved stable disease (SD). Confirmed PR was observed in 11 patients (33%) (Supplementary Table 2). No patient achieved CR. Six patients showed disease progression (PD) at the time of the first CT scan. One patient died after 1 treatment cycle without CT assessment. The confirmed ORR was 33% ($n = 11$), and the disease control rate (DCR) was 79% ($n = 26$). Tumor shrinkage was observed in 24 patients (73%) (Fig. 2A). For the 11 patients who achieved confirmed ORR, the median time to response was 2.0 months and the median duration of response was 6.2 months (Fig. 2B, C). The median PFS was 7.3 months (95% CI, 5.6–8.6), and the median overall survival (OS) reached 17.4 months (95% CI, 15.9-not reached [NR]). The 6-month PFS rate was 60%, and the 1-year OS rate was 85% (Fig. 2D, E).

Twenty-nine (88%) patients have failed in the previous cetuximab-containing therapy. Four patients who had never used cetuximab but had failed on other second- or third-line treatment previously were included in this study. Of the 4 cetuximab-naïve patients, only one reached PR, while for the 29 cetuximab-exposed patients, 10 patients reached PR. No statistical differences in PFS or OS were observed between the two groups (PFS: 8.2 months for Cetuximab-naïve patients vs 6.8 months for Cetuximab-exposed patients, $P = 0.87$; OS: NR for Cetuximab-naïve patients vs 17.4 months for Cetuximab-exposed patients, $P = 0.41$) (Supplementary Fig. 2A, B). Of the 29 Cetuximab-exposed patients, 7 experienced treatment failure on their previous regimens containing Cetuximab and enrolled in our study without a period of Cetuximab-free time. Of these 7 patients, 2 achieved PR after the addition of ICI, and 4 had SD, with one of them controlling the disease for over 2 years.

Liver or lung metastasis may serve as a biomarker for ICIs, we hence evaluated the efficacy of treatment between patients with or without liver or lung metastasis. As shown in Supplementary Fig. 1, the ORR was comparable between patients with liver metastasis (10/26, 38.5%) and those without liver metastasis (2/6, 33.3%) using Fisher's exact test ($P > 0.99$). However, the PFS trended shorter in patients with liver metastasis (6.1 months *vs* 8.6 months; $P = 0.38$), but no significance was reached. The mPFS (6.8 with lung metastasis vs 7.3 months without lung metastasis; $P = 0.17$) were also not significantly different between patients with or without lung metastasis, although patients without lung metastasis tended to have higher ORRs (4/19 [21.1%] with lung metastasis vs 8/14 [57%] without lung metastasis, $P = 0.07$). More details of the subgroup analysis are provided in Supplementary Fig. 1.

Safety

The median number of treatment cycles was 12 per patient (range, 1–42 cycles). The median exposed dose of tislelizumab, cetuximab, and irinotecan was 2400, 8800, and 2400 mg per patient, respectively. Among the 33 treated patients, 32 patients (97%) had treatment-related AEs (Fig. 2F and Supplementary Table 3). No grade 4/5 AEs were reported. Immune-related AEs included 2 grade 1 hyperthyroidism, 3 grade 1 hypothyroidism, and 1 event each of grade 2 immune dermatitis and myocarditis, which improved after the treatment with thyroxine or corticosteroids.

https://doi.org/10.1038/s41467-024-51536-x

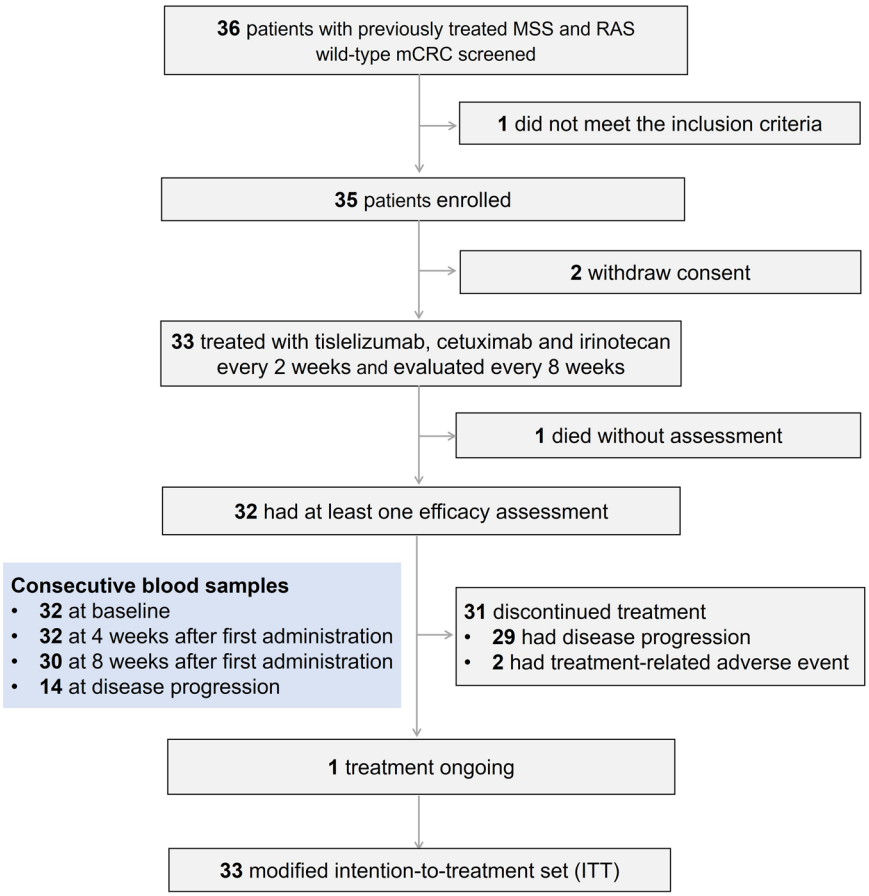

Fig. 1 | Study flow. After excluding 1 patient who didn't meet the inclusion criteria and 2 patients who withdrew their consent, 33 patients were treated with TEC regimen, and included in the modified intention-to-treatment set (mITT) analysis.

Treatment was delayed in 68 cycles (17%) because of an AE, and it was related to cetuximab and irinotecan in 25 and 39 cycles, respectively. The cetuximab dose was reduced in 9 patients (27%) due to rash, and irinotecan dose was reduced in 11 patients (33%) due to diarrhea or hematologic toxicity or vomiting. A total of 29 patients (88%) received a further line of treatment after disease progression.

ctDNA metrics were associated with the clinical benefit

Similar ultimate outcomes were observed between the patients who achieved PR or SD (Supplementary Fig. 2C, D). Therefore, we defined patients with non-PD (SD or PR) as responders and sought to find another way to identify the patients who would eventually benefit from the TEC regimen. The post-hoc analysis of ctDNA used the mean VAF as a continuous metric of ctDNA concentration. Overall, ctDNA was detected in all patients (100%, 32 of 32) at baseline, with *TP53* (81%), *APC* (69%), and *CARD11* (16%) being the most abundant alterations (Supplementary Fig. 3A). Patients with a lower VAF (below the median) had longer OS compared with those with a higher VAF (above the median) at baseline (Fig. 3A, HR: 4.95, 95% CI, 1.71–14.29; $P = 0.0058$). Patients with PD ($n = 6$) had a higher VAF than non-PDs (SD + PR, $n = 26$) at all time points (Fig. 3B). The TEC treatment reduced the VAF 4 weeks (C2D15) after initiation in most patients, particularly in responders, regardless of PR or SD (Fig. 3B–D). By employing ROC curve and Youden index analysis, we determined the optimal cutoff value for VAF decrease from pretreatment and classified patients into two groups: with or without ctDNA molecular response. Patients with ctDNA molecular responses at T2 (Fig. 3E, HR = 3.12; $P = 0.024$) or T3 (Fig. 3F, HR = 5.20; $P = 0.042$) both had significantly longer OS. Accordingly, patients with lower ctDNA levels (VAF < 1%) and evaluated at every time point (T2, T3, T4) had much longer OS than those with higher ctDNA levels (VAF ≥ 1%) (Supplementary Fig. 4A). A similar trend for PFS was also observed (Supplementary Fig. 4B).

The mean VAF was positively correlated with tumor size at similar time points (Fig. 3G; Supplementary Fig. 4C, D). Moreover, the percent change in the mean VAF from T1 (pretreatment) to T2 (C2D15) or T3 (C4D15) correlated with the tumor shrinkage from baseline to week 8 as assessed by CT (R = 0.54, $P = 0.0013$, Fig. 3H; Supplementary Fig. 4E). Notably, in contrast to the overlapped Kaplan-Meier (KM) curves for patients with conventional radiographic SD and PR (Supplementary Fig. 2C, D), the patients who achieved ctDNA molecular response tended toward better OS compared with those who did not (HR: 3.15; $P = 0.059$, Supplementary Fig. 4F), indicating ctDNA may be more sensitive than radiographic tumor assessment for risk stratification among responders. For 13 responders who had blood samples available for all 4 time points, visualizing ctDNA dynamics parallel to the tumor size dynamics revealed that ctDNA changes mirror tumor size changes (Fig. 3I, J). Moreover, plasma TMB at T2 and T3, but not T1, showed a significant difference between PD and non-PD (Supplementary Fig. 4G).

Besides, we found 6 patients evolved into *RAS* mutation ($n = 3$) or *BRAF* mutation ($n = 3$) in baseline ctDNA. One patient with *KRAS* mutation detected at baseline even achieved partial response. This specific mutation site was KRAS Q61H, but it is worth noting that the mutation frequency in this case was quite low. Both the median OS (12.0 months vs 18.0 months, HR: 4.60, 95% CI, 1.06–9.92; $P = 0.026$; Fig. 3K) and median PFS (3.9 months vs 8.0 months, HR: 3.90, 95% CI, 1.25–12.17; $P = 0.012$; Supplementary Fig. 4H) were significantly shorter in patients with *RAS/BRAF* MUT compared with patients with *RAS/BRAF*

Table 1 | Baseline and Demographic and Clinical Characteristics of Patients (*n* = 33)

	n (%)
Median age, years (range)	58 (35–80)
≥65 years	10 (30%)
<65 years	23 (70%)
Sex	
Male	24 (73%)
Female	9 (27%)
Primary tumor site	
Left	32 (97%)
Right	1 (3%)
ECOG performance status	
0	6 (18%)
1	27 (82%)
Number of metastatic organs	
1–2	20 (61%)
≥3	13 (39%)
Liver metastasis	
Yes	26 (79%)
No	7 (21%)
Lung metastasis	
Yes	19 (58%)
No	14 (42%)
Time since diagnosis of the first metastasis, months, median (range)	30 (10–72)
Number of prior regimens	
2	11 (33%)
3	17 (52%)
≥4	5 (15%)

WT. For ctDNA status evaluated at the time of progression for responders, many secondary mutations, including *EGFR* (*n* = 6), *KRAS* (*n* = 5), *MAP2K1* (*n* = 3), *HMCN1* (*n* = 2), and *KDM5A* (*n* = 2), were detected (Supplementary Fig. 3B).

Dynamics of plasma immune proteomics are associated with the response to TEC

Post-hoc proteomic analysis revealed that a global increase of almost all markers was found in responders (non-PD) at baseline (Fig. 4A, B and Supplementary Fig. 5A). The 26 identified statistically significant proteins (Fig. 4A, B) were inextricably interacted (Fig. 4C), and most of them were correlated with PFS (Fig. 4D). Pathways involving innate and adaptive immunity, such as "Positive regulation of lymphocyte-mediated immunity," "Response to chemokines," and "Neutrophil migration," were more enriched in responders (Fig. 4E).

Furthermore, TEC treatment also induced an increased expression of most plasma proteins at T2 (C2D15) and T3 (C4D15), irrespective of the response (Fig. 4F, G). However, at the time of progression, more than half of the plasma proteins were decreased (Fig. 4H and Supplementary Fig. 5B). Their functions were mainly enriched in pathways associated with "cell chemotaxis," "cytokine activity," and "response to biotic stimulus" (Supplementary Fig. 5C–E). Pathways such as "Neoplasm," "Breast cancer basal up," and "Abnormality of the lymphatic system" were activated in comparisons between T4 (progression) and T3 (C4D15). We chose 10 proteins (Fig. 4I) that changed in both T2 and T3 in comparison with T1 (indicating a robust and lasting activation after TEC treatment) and found most of them also correlated with OS and PFS (Supplementary Fig. 5F), especially at the time of T3 (C4D15). The level of soluble PD-L1 expression was similar between non-PD and PD at all time points that were assessed (Supplementary Fig. 5G).

We also endeavored to establish a score system to quantify the peripheral immune proteomics in a global manner to reveal the intensity of the PME's "hot" or "cold" nature. As shown in Fig. 4J, the survival probability of patients with high protein scores was longer than those with low protein scores (HR: 0.306, 95% CI, 0.1–0.9; $P = 0.031$).

Negative correlation between plasma immune proteomics and ctDNA metrics and prognosis for MSS mCRC

A negative correlation was observed between plasma proteomics and ctDNA metrics after TEC treatment. All the 25 significant elevated proteins in responders at baseline and key ctDNA metrics after TEC treatment, including ctDNA levels at T2, ctDNA levels at T3, and decreases in ctDNA levels at T2 or T3, were all negatively correlated (Fig. 5A). In line with it, patients with ctDNA molecular responses at T2 showed an increase of several immune markers compared with baseline (Fig. 5B). Subsequently, we performed a univariate Cox regression analysis of factors including clinicopathologic variables, key ctDNA features, and peripheral immune protein levels. As shown in Fig. 5C, ctDNA metrics, such as ctDNA levels or reduction in ctDNA levels and proteomics scores at baseline and T3, were associated with OS. Furthermore, we selected variables with a *P*-value < 0.1 in the univariate analysis to be included in the multivariate Cox regression analysis. As illustrated in Fig. 5D, after adjusting for those confounding factors, ΔctDNA (T2-T1) and proteomics scores at T1 were still independent factors related with OS.

Discussion

In this study, we reported that tislelizumab plus cetuximab and irinotecan (TEC) met its primary endpoint with an ORR of 33% in patients with MSS and *RAS* WT refractory mCRC. The mPFS was 7.3 months and the mOS was 17.4 months, which are exponentially favorable to the historical standard salvage-line therapies including regorafenib[3], fruquintinib[30], or trifluridine-tipiracil[4]. This study also included a translational analysis of serial liquid biopsies. We found that pre-treatment ctDNA levels (VAF) and on-treatment VAF reductions were associated with the response of TEC. Moreover, the levels of most immune-oncology proteins were higher in responders, and the patients with high proteomics scores at baseline were associated with better OS (Fig. 6). Importantly, a negative association between the peripheral immune proteomics and ctDNA metrics was observed, indicating the wax and wane of the host systemic immunity and tumor dynamics.

Although only a limited number of relatively small size studies have been published so far, the combination of EGFR antibody with irinotecan in the third-line setting has shown an ORR ranging from 3% to 23% and mPFS ranging from 2.4 months to 5 months[5,31–33]. For instance, the CRICKET study[5] showed that a rechallenge with cetuximab and irinotecan achieved an ORR of 21% (confirmed ORR, 14%), mPFS of 3.4 months, and mOS of 9.8 months in the third-line setting for mCRC (*n* = 28). In another cohort with larger sample size (*n* = 218), patients with non-*RAS*-selected and irinotecan-refractory CRC, cetuximab plus irinotecan reported an ORR of 23% with PFS of 4.1 months[31]. In this study, the confirmed ORR of the TEC regimen was 33%, the median OS was 17.4 months, and the median PFS was 7.3 months. The triplets in TEC exceeded the efficacy of the doublet of re-treatment with cetuximab in combination with irinotecan. CHRONOS study[6] showed an exceptional ORR of 30% (confirmed ORR 22%) for panitumumab rechallenge, but it specifically selected patients with 'zero mutation ctDNA triage' at baseline. In our study, for the patients with confirmed *RAS/BRAF* WT in the baseline ctDNA, the triplets (confirmed ORR: 38%, mPFS: 8.0 months, and mOS: 18.0 months) exceeded the single panitumumab in CHRONOS[6] (confirmed ORR: 22% and mOS: 13.8 months). It also exceeded the doublets in the CRIKET study[5] in the RAS/BRAF WT population (cetuximab plus irinotecan; confirmed ORR:

https://doi.org/10.1038/s41467-024-51536-x

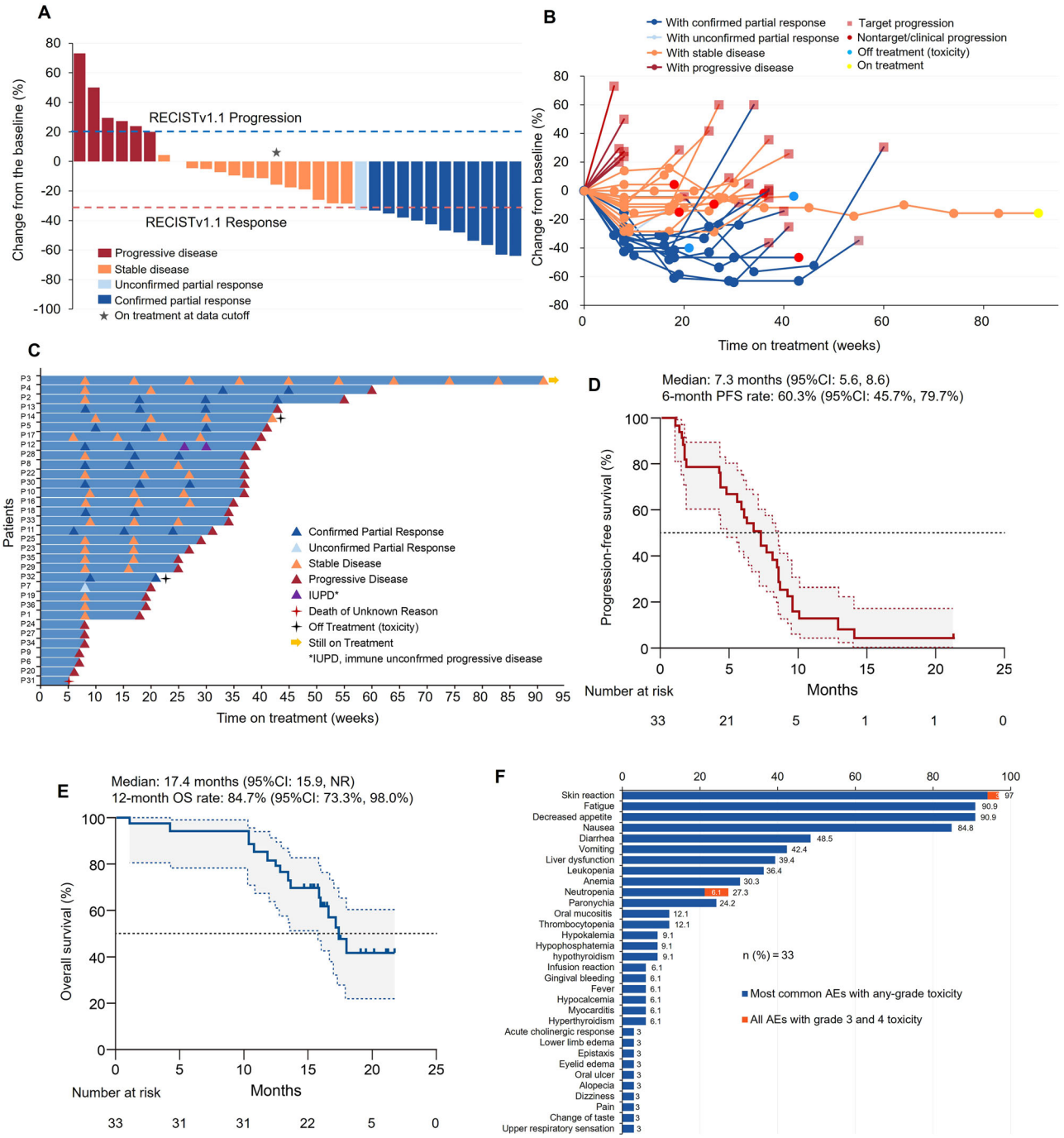

Fig. 2 | Tumor response. Waterfall plot shows the maximum percent change from baseline in the sum of the longest diameters of target lesions in 32 patients who were treated in the current study and underwent radiologic evaluation. **A** Spider plot shows the change in sum of the target lesion diameters over time ($n = 32$). **B** Swimmer plot shows the duration of treatment ($n = 33$). **C** Kaplan-Meier plot of progression-free survival. **D** Kaplan-Meier plot of overall survival. NR not reached. **E** Frequency of AEs. Source data are provided as a Source Data file.

31%, mPFS: 4.0 months, and mOS: 12.5 months). These data indicated that the addition of ICIs into the combination may have better efficacy, despite cross-trial comparisons require careful interpretation.

Notably, out of the 29 patients who had previously been exposed to Cetuximab, 7 were promptly enrolled in this study following Cetuximab resistance without any interval. Nevertheless, 6 of these 7 patients achieved disease control after the addition of ICI. Therefore, PD-1 blockade may have additive or synergetic effects with Cetuximab, even in patients with Cetuximab resistance. Theoretically, Cetuximab may change the immune microenvironment through cross talk with immune cells or increasing the expression of immune checkpoints[11–17]. This has been proved in patients with recurrent or metastatic head and neck squamous cell carcinoma[18]. In patients with mCRC, the CAVE study[19] (avelumab plus cetuximab; ORR: 7.8%, mPFS: 3.6 months, and mOS: 11.6 months) or NCT02713373[34] (pembrolizumab plus cetuximab; ORR: 2.6%, mPFS: 4.1 months, and mOS: 14.5 months) showed a slight advantage; however, the results were not encouraging. Therefore, we hypothesized that chemical agents may exert a significant effect on the combination, which could sensitize unresponsive tumors by engaging the immune cells to infiltrate the TME[20,21]. Cohort B of the phase 2 CRACK study[35], along with our study, represented that the triplets, including PD-1 antibody (camrelizumab or tislelizumab)

https://doi.org/10.1038/s41467-024-51536-x

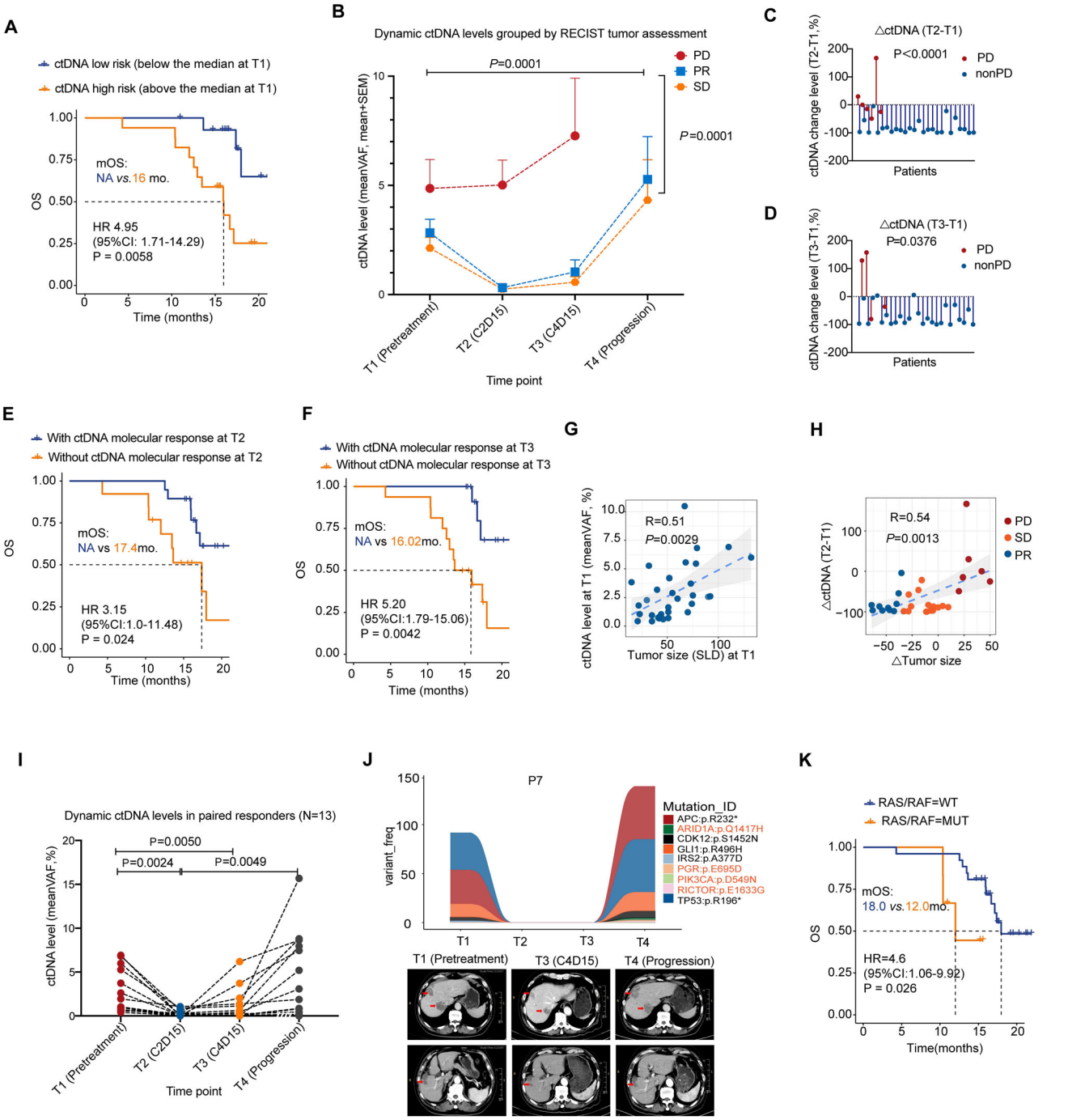

Fig. 3 | Dynamic ctDNA levels associated with clinical outcomes. A Kaplan-Meier analysis showing the prognostic value of pretreatment ctDNA for OS, where the orange curve indicates patients with ctDNA levels greater than or equal to the median (≥2.1%, $n = 16$), and the blue curve indicates patients with ctDNA less than the median ($n = 16$). **B** Dynamic changes of ctDNA levels before and on treatment. Mixed-effects model was used to derive p-values. ($n = 12$ for PR, $n = 14$ for SD, $n = 6$ for PD). **C** ctDNA level changes at T2 between non-PD (n = 26) and PD (n = 6). Two-tailed Mann-Whitney U test was used to derive P-value. The exact P-value indicated by '$P < 0.0001$' is 6.6×10^{-5}. **D** ctDNA level changes at T3 between non-PD ($n = 26$) and PD ($n = 4$). Two-tailed Mann-Whitney U test was used to derive P-value. **E** KM curves showing OS for patients with ctDNA molecular response ($n = 19$) versus patients without ctDNA molecular response ($n = 13$) at T2. The optimal cutoff value for ctDNA decrease was calculated by ROC curve and Youden index analysis. And the threshold is set at a 83.44% reduction from pretreatment. **F** KM curves showing OS for patients with ctDNA molecular response ($n = 14$) versus patients without ctDNA molecular response ($n = 16$) at T3. The optimal cutoff value for ctDNA decrease was calculated by ROC and Youden index analysis. And the threshold at T3 is 82.57% reduction from pretreatment. **G** Correlation of ctDNA levels at T1 and tumor size at baseline. Pearson correlation test was used ($n = 32$). **H** Correlation of ctDNA level changes at T2 and radiographic assessment at week 8. The percent change in tumor size was evaluated as the sum of longest diameters (SLD). Pearson correlation test was used ($n = 32$). **I** Dynamic changes of ctDNA levels for patients with available biopsies at all time points ($n = 13$). Two-tailed paired t-tests were used to derive P-value. **J** The ctDNA landscape changes (upper panel) and the representative radiographic images of tumors (bottom panel) for patient #7 at different time points. **K** Overall survival in patients with baseline ctDNA *RAS/BRAF* mutational status. ($n = 26$ for *RAS/BRAF* WT, $n = 6$ for *RAS/BRAF* MUT). For (**A**, **E**, **F**, **K**), a univariable Cox proportional hazards model was used to estimate the HR and logrank test was used to report P-value. Source data are provided as a Source Data file.

https://doi.org/10.1038/s41467-024-51536-x

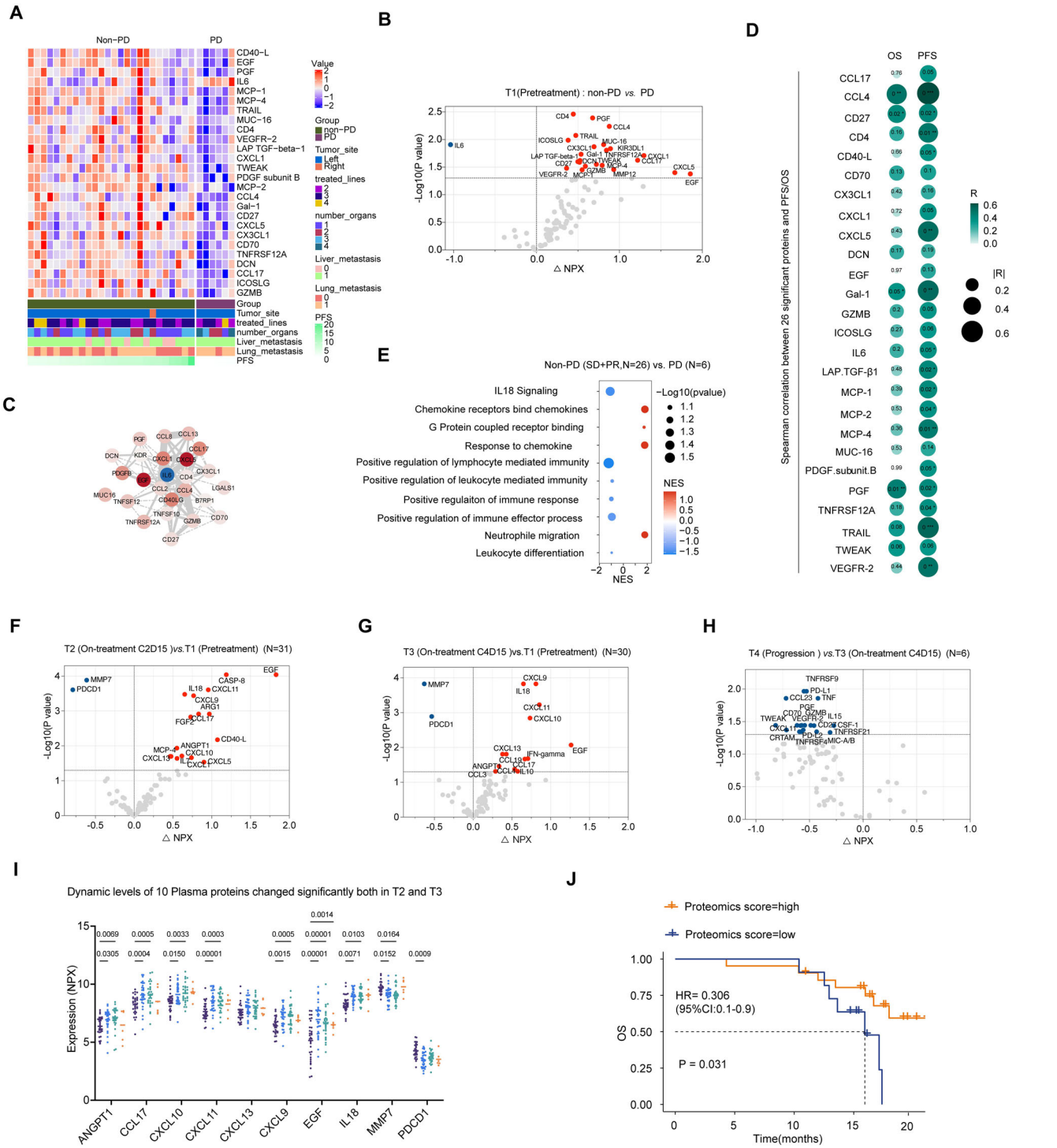

Fig. 4 | Dynamics of plasma immune proteomics are associated with the response to TEC. A Heatmap showing the expression of 26 significantly changed proteins between the non-PD group ($n = 26$) and PD group ($n = 6$) at baseline. **B** Volcano plots showing differential expression of plasma proteins between the non-PD ($n = 26$) and PD ($n = 6$) at baseline. **C** The interaction of 26 proteins in (**A**) analyzed by Cytoscape. The color of the nodes shows the changes in protein levels between the non-PD and PD (ΔNPX). The thickness of lines between the nodes indicates the co-expression degree of 2 proteins linked. **D** The Spearman correlation between 26 significant proteins and PFS/OS ($n = 32$). **E** GSEA analysis of significant proteins identified in (**A**). **F** Volcano plots showing differential expression of plasma proteins between T2 (on-treatment C2D15) and T1 (pretreatment), $n = 31$. **G** Volcano plots showing differential expression of plasma proteins between T3 (on-treatment C4D15) and T1 (pretreatment), $n = 30$. **H** Volcano plots showing differential expression of plasma proteins between T4 (time of progression) and T3 (on-treatment C4D15), $n = 6$. **I** Dynamic changes of 10 plasma proteins significantly changed both in T2 and T3. Dunnett's multiple comparisons test was used. *P*-value was adjusted, $n = 30$. **J** KM curves of OS for patients with high ($n = 21$) or low proteomics scores ($n = 11$). A univariable Cox proportional hazards model was used to estimate the HR and logrank test was used to report *P*-value. For volcano plots, the horizontal axis displays the magnitude of a protein's change; the vertical axis displays the significance scale by the $-\log_{10}$ (*P*-value), which increases with statistical significance. For (**A**), two-tailed Wilcoxon rank sum test was used. For (**B**, **F**, **G**, **H**), two-tailed paired t-test was used. *P*-value was adjusted by Benjamini-Hochberg method. The horizontal black dotted line corresponds to the *P*-value cutoff of 0.05. Red dots are biomarkers with a significant upregulation and blue dots are biomarkers with a significant downregulation. Source data are provided as a Source Data file.

https://doi.org/10.1038/s41467-024-51536-x

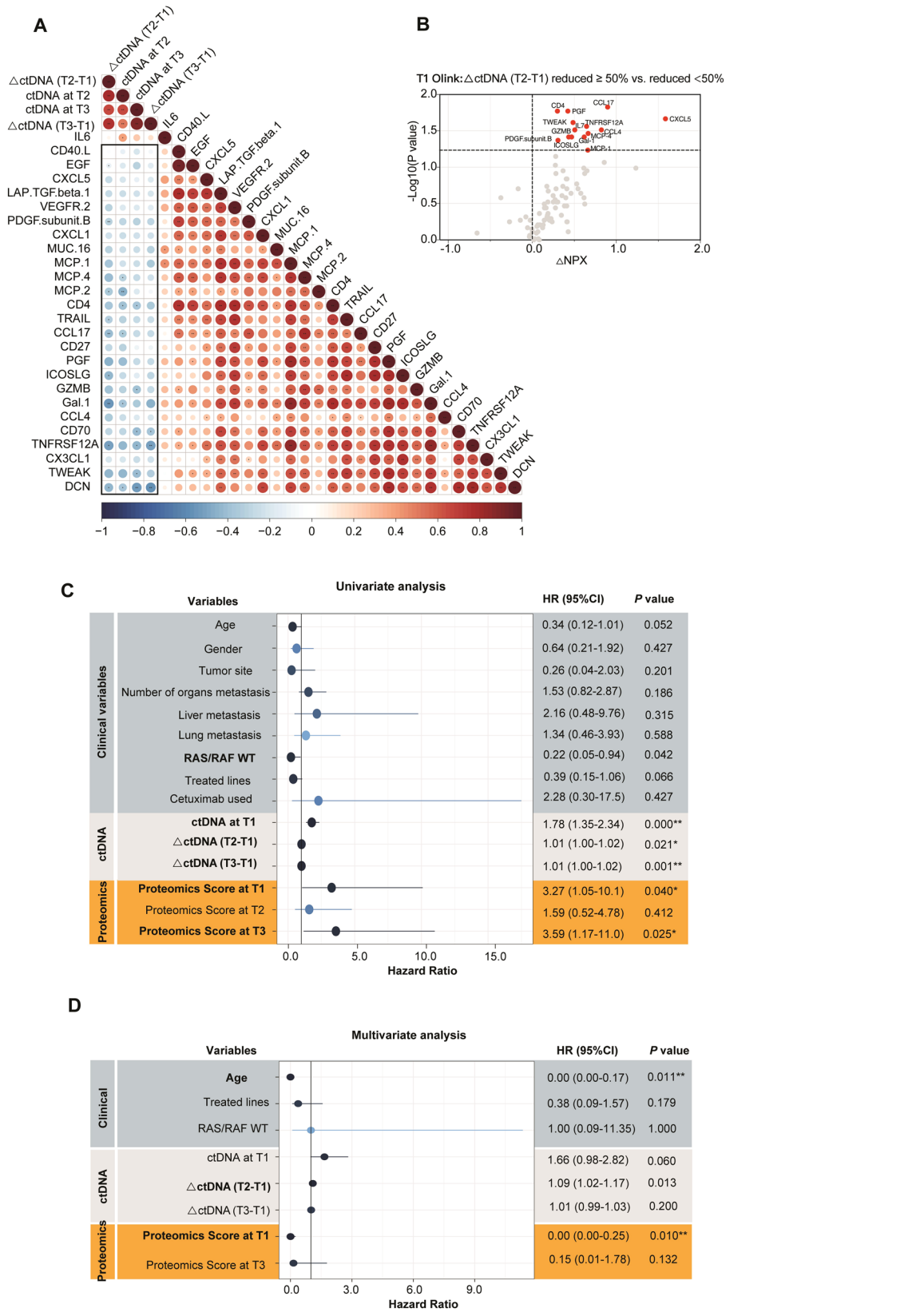

Fig. 5 | Correlation between ctDNA metrics and PME. A The Pearson correlation between the ctDNA metrics and plasma immune markers, $n = 32$. **B** Volcano plots showing differential expression of plasma proteins between ΔctDNA (T2-T1) ≥ 50% versus < 50%. Two-tailed paired t-test was used. *P*-value was adjusted by Benjamini-Hochberg method, $n = 32$. **C** Univariate Cox regression analysis of different variables for OS of patients. Note: bold indicates significant difference with $P < 0.05$. Horizontal lines represent the 95% confidence interval of HR, $n = 32$. **D** Multivariate Cox regression analysis of different variables for OS of patients. Note: bold indicates significant difference with $P < 0.05$. Horizontal lines represent the 95% confidence interval of HR, $n = 32$. Source data are provided as a Source Data file.

https://doi.org/10.1038/s41467-024-51536-x

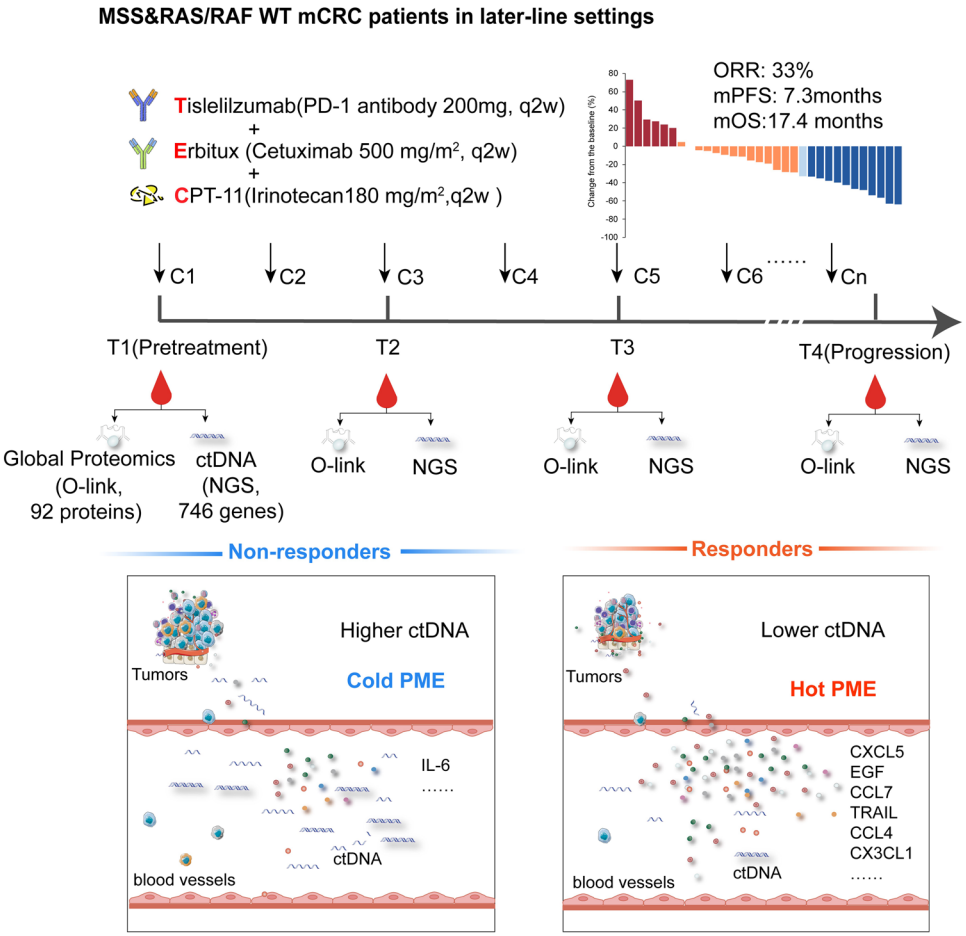

Fig. 6 | Schematics of TEC administration and its efficacy. Tislelizumab plus cetuximab and irinotecan (TEC) met its primary endpoint with an ORR of 33% in patients with MSS and *RAS* WT refractory mCRC. The mPFS was 7.3 months and the mOS was 17.4 months. Pretreatment ctDNA levels and immune-oncology proteins levels were associated with the response. (Adobe Illustrator CS5 software).

combined with cetuximab and irinotecan, may work synergically and exceed the efficacy of the doublets of cetuximab in combination with irinotecan or with ICIs. TEC has the potential to be a treatment option for MSS and *RAS/BRAF* WT mCRCs in the later-line settings if validated in larger trials.

Previous studies such as REGONIVO[36], C800 trial[37] and RIN[38] therapy have shown that patients with liver metastasis tend to have a weaker response to immunotherapy, while those with lung metastasis may experience better efficacy. We also found the PFS trended shorter in patients with liver metastasis than those without liver metastasis despite a comparable ORR. Additionally, the mPFS was not significantly different between patients with or without lung metastasis, although patients without lung metastasis tended to have higher ORRs. When combined with EGFR antibody, ICIs may exhibit varying responses compared to ICIs combined with anti-angiogenic agents in patients with liver or lung metastasis. Further research using larger sample sizes is necessary to fully understand the predictive role of liver or lung metastasis on the effectiveness of immunotherapy.

The safety profiles for TEC were expected and manageable, based on the toxicity profile of each drug, and no new AEs were identified for the combination. Moreover, in contrast to the high incidence of grade 3/4 treatment-related AEs (ranging from 27% to 87%)[36,39,40] with the administration of antiangiogenic tyrosine kinase inhibitors with or without ICIs, TEC was well tolerated. No serious or unexpected AEs were reported. Notably, the recommended dose of tislelizumab is 200 mg every 3 weeks, but we used 200 mg tislelizumab every 2 weeks in this study after deliberating the pharmacokinetics, safety, and efficacy data for tislelizumab obtained from human studies. The findings revealed that the dose was safe and efficacious. Only seven mild immune-related AEs were reported, which were manageable with the treatment with thyroxine or corticosteroids. A total of 29 patients (88%) received a further line of treatment after progression in this study, indicating a good performance was still maintained after TEC treatment.

By incorporating longitudinal ctDNA evaluation of paired pre- and on-treatment liquid biopsies from nearly all patients, our study demonstrated that the total amount of ctDNA levels were correlated with total disease burden and that ctDNA metrics collected across longitudinal time points can be used to risk stratify the patients and predict the survival. On-treatment ctDNA dynamics may predict the OS more accurately and earlier than traditional CT scans. This was consistent with the findings from prior studies showing that ctDNA can be used effectively to monitor the response to cancer therapy[25,26,41,42]. Another study showed that ctDNA dynamics after just a single infusion can aid in the identification of patients who will achieve durable clinical benefits[42]. Hence, early ctDNA molecular response appears to be a promising approach for early response assessment and prediction of ultimate clinical benefit more precisely. Another superiority and irreplaceability of ctDNA over radiographic imaging is that serial genomic profiling of ctDNA could provide a real-time comprehensive characterization of clonal evolution, particularly the emergence of mutations of acquired resistance in patients treated with anti-EGFR therapy. The concordance between the detection of mutations in tissue and plasma has extensively been demonstrated. We also identified 6

patients with secondary *RAS/BRAF* mutations in ctDNA at baseline, and most of these patients indeed had quite poor response to TEC treatment. With the rapid improvement of ctDNA sequencing technology, ctDNA offers a promising option to characterize the course of mCRC in a minimally invasive way to guide the treatment of the patient.

In contrast to the extensively studied local immunity in the TME, little is known about the relationship between the systemic immunity and immunotherapy response in mCRC, yet immunity is coordinated across tissues. The localized antitumor immune response cannot exist without continuous communication with systemic immunity. Therefore, a thorough understanding of immune responses to cancer should include immunity across the peripheral immune system in addition to within the TME. In this study, by performing parallel studies with matched plasma biopsies from the same patients, we screened circulating immune protein expressions in the spectrum of responders and nonresponders using a DNA oligonucleotide-based Olink immunoassay. We identified immune signatures in responders and over the treatment continuum. It was found that responders had ubiquitously higher expression of most immune proteins that belonged to the pathways involved in both innate and adaptive immunity. TEC treatment increased the expression of the majority of plasma immune proteins. The global immune environment in blood was defined as PME, with the presumption that a hot PME may have the association with the responses. Moreover, we developed a scoring system to quantify the peripheral immune proteomics and demonstrated that patients with high proteomics scores at baseline had better OS. Consistent with our observation, another study also found a significant increase in almost all immune-oncology-related plasma proteins after neoadjuvant immunotherapy in melanoma[43].

Interestingly, we found a negative association between the peripheral immune proteomics and ctDNA levels, perhaps a reflection of the "seesaw" effect between the tumor and host systemic immunity. By using multivariate Cox regression analysis, we further integrated clinical and translation data in our study to predict the response and stratify the risk. This model was not limited only to static features of pretreatment tumors but also encompassed dynamic biomarkers that capture the tumor evolution under the selective pressure of ICI-based therapy. Significant intratumoral heterogeneity of colorectal cancer and limited biopsy depth largely impair the representation of biopsy samples. Comparably, peripheral immune proteomics and ctDNA metrics incorporate both systemic and local features for hosts and tumors and are thus sensitive and informative.

This study was limited by its single-arm single-center design and small sample size. The definition of PME would be better when taking immune cells ratios and function into consideration. The value of ctDNA and global immune proteomics deserve to be further explored and validated. Nevertheless, the study showed encouraging antitumor activity of TEC and could be a promising therapeutic option for advanced mCRC. A randomized, multicenter, controlled clinical trial (NCT05278351) of tislelizumab plus cetuximab and irinotecan versus third-line standard of care in refractory MSS mCRC is currently ongoing, in order to validate the results of this study.

In conclusion, tislelizumab in combination with cetuximab and irinotecan showed an encouraging clinical efficacy and tolerable safety profile in previously treated patients with MSS and *RAS* WT mCRC. Peripheral immune profiling and ctDNA offer a promising, noninvasive approach to monitor the therapeutic efficacy in real time.

Methods

Study design and participants

This was an open-label, single-arm, single-center, phase 2 study. The study was approved by the ethics committee of the Zhongshan Hospital affiliated to Fudan University (Approval Number B2020-344) and was conducted in accordance with the principles of the Declaration of Helsinki and the International Conference on Harmonization and Good Clinical Practice guidelines. The major inclusion criteria included (1) histologically confirmed advanced or metastatic MSS and *RAS* WT colorectal adenocarcinoma refractory to at least 2 previous lines of therapy, (2) an Eastern Cooperative Oncology Group performance status score of 0 or 1, and (3) adequate hematologic, hepatic, and renal functions. The key exclusion criteria included (1) patients with dMMR or MSI-H; (2) *RAS* or *BRAF* mutation detected in any previous tissue samples; (3) previous treatment with immunotherapy, such as anti-PD-1, anti-PD-L1, anti-cytotoxic T-lymphocyte–associated antigen 4, or any immunocytes therapy; (4) active autoimmune diseases; or (5) serious comorbidity. Sex or gender were not considered in the study design. Tislelizumab was administered at a fixed dose of 200 mg in combination with cetuximab at a dose of 500 mg/m^2 and irinotecan at a dose of 180 mg/m^2 every 2 weeks until disease progression (PD) or the development of unacceptable toxicity. Dose modifications of tislelizumab were not permitted. Modifications to the doses of cetuximab and irinotecan were made according to the drug instructions. Interruptions in the doses were allowed according to the severity of AEs. All participants provided written informed consent for participating in this study and publishing clinical information. There was no additional compensation for patients. This trial was preregistered at https://www.chictr.org.cn/ with identifier of ChiCTR2000035642 on August 15th, 2020, and retrospectively registered at ClinicalTrials.gov with identifier of NCT05143099 on November 22nd, 2021. The study protocol is available in the Supplementary Information file.

Assessment

Tumor response was evaluated every 8 weeks using computed tomography (CT) or magnetic resonance imaging (MRI). Investigators performed the assessment using the Response Evaluation of Criteria in Solid Tumor 1.1 (RECIST1.1). For patients who progressed for the first time, another 2 cycles of treatment followed by a repeat CT assessment were allowed according to the immune RECIST (iRECIST) criteria. AEs were assessed from the date of initiation of protocol therapy until 28 days after the administration of the last dose according to the National Cancer Institute's Common Toxicity Criteria for Adverse Events (version 5.0).

Outcomes

The primary endpoint was ORR, which was defined as the proportion of patients with the best response of complete response (CR) or partial response (PR). The PR was considered as confirmed only if PR was maintained and observed on 2 consecutive scans. Patients whose disease was not reassessed and those who were unavailable for the follow-up were considered as nonresponders for the primary endpoint analysis. The secondary endpoints included DCR, PFS, and OS. DCR was defined as the proportion of patients achieving CR, PR or SD. PFS was defined as the duration from the treatment initiation to PD or death as a result of any cause, whichever occurred first. OS was defined as the duration from the treatment initiation to death. ORR, DCR, and PFS were assessed using the iRECIST criteria. The exploratory objective was to examine the biomarkers for clinical activity through consecutive blood samples.

ctDNA evaluation by NGS

The consecutive blood samples were prospectively collected at baseline (T1, pretreatment), 4 weeks after the first administration (T2, C2D15), first assessment at 8 weeks (T3, C4D15), and PD (T4, progression) for post hoc analysis. Approximately, 16 to 20 mL of blood was collected in EDTA tubes and centrifuged at 4 °C for 10 minutes at 200 g within 30 minutes after the collection of blood. Plasma samples were stored at −80 °C until analysis. Circulating free DNA was extracted using a MagMAX™ Cell-Free DNA Isolation Kit (Thermo Fisher Inc) from plasma following the manufacturer's protocol. Peripheral blood mononuclear cell was treated as normal control to filter the germline

mutations, and DNA was extracted using TIANamp Blood DNA Kit (TIANGEN). Genomic DNA was fragmented to a length of about 200 bp using Covaris LE220, starting from an input amount of 30 to 300 ng. The libraries were prepared by KAPA HyperPrep PCR-free Kit (KAPA). The next-generation sequencing was performed using a panel encompassing 769 cancer-related genes. The hybridized library was subjected to sequencing on the Illumina NovaSeq 6000 platform using paired-end 150 bp mode. Tumor mutational burden (TMB) was reported as the number of somatic mutations per megabase (mut/Mb) of the captured region. The mean variant allele frequency (VAF) was calculated as the average VAF based on the identified mutations that met the criteria for reliability, which was the representative of the ctDNA levels in this study. Details about variant calling, somatic mutation filtering, and monitoring are in the supplementary materials.

Plasma proteomics profiling using olink proximity extension assay technology

Thirty-two pretreatment (T1), 31 on-treatment C2D15 (T2), 30 on-treatment C4D15 (T3), and 6 at progression (T4) plasma samples from patients with TEC treatment were suitable for testing. A multiplex assay to profile the plasma proteomics was performed using proximity extension assay (PEA) technology (Olink Bioscience AB), according to the manufacturer's instructions. We selected the Olink® Target 96 Immuno-Oncology panel (Olink Proteomics AB, Uppsala, Sweden) that included 92 key unique markers. The PEA technology used for the Olink's protocol has been well described[27,44,45]. In summary, the basis of PEA is a dual-recognition immunoassay. Two matched antibodies labeled with unique DNA oligonucleotides simultaneously bind to a target protein in solution. Once the antibodies bind to a target protein, the 2 antibodies would be placed in proximity, allowing their DNA oligonucleotides to hybridize and serve as a template for a DNA polymerase-dependent extension step. The hybridized DNA creates a double-stranded DNA "barcode," which is unique for the specific antigen and quantitatively proportional to the initial concentration of the target protein. The hybridization and extension are immediately followed by PCR amplification and qualification. All assay validation data (detection limits, intra-assay precision data, inter-assay precision data, etc.) are available on the manufacturer's website (www.olink.com). The protein levels were presented in the form of normalized protein expression (NPX). Proteins that were below the detection limit in over 80% of the samples were excluded from further analysis. The full plasma proteomics dataset is available in the Source Data file.

An attempt to quantify the peripheral immune proteomics globally was made to indicate the "hot" or "cold" extent of the peripheral macroenvironment (PME). As no scoring system is available for proteomics evaluated by the Olink platform, insights from gene studies were used to devise a scoring method in this study. We defined the regression coefficient (β) for each protein, which was obtained from the coef parameter in the DESeq2 function. A per-sample weighted plasma immune proteins score was calculated by multiplying the expression value of each protein with its corresponding β coefficient, followed by z-score normalization[46]. The formula was as follows:

$$\text{protein score} = \sum_{i=1}^{n} \beta_i * \text{protein}_i \quad (1)$$

where i ranges from 1 to number of proteins assessed and β corresponds to the beta coefficient of the respective protein obtained from the coef parameter in the DESeq2 function. A 0.33 quantile cutoff was used to divide patients into high or low expression groups based on their corresponding weighted protein score.

Statistical analysis

According to Simon's minimax two-stage design with a power of 0.9 and one-sided α of 0.05 and assuming that the poor ORR (ineffectiveness, P0) was 10% compared with the good ORR (effectiveness, P1) of 30%, the sample size required for the first stage was 22. If the number of patients achieving objective response was >2, the study proceeded to the second stage. In stage 2, 11 more patients were planned to be enrolled. A total of 33 patients was included, and the primary endpoint was considered met if >6 patients achieved an objective response. Considering a possible 5% dropout rate of patients, a total of 35 patients were enrolled in the study.

Patients who received at least 1 cycle of treatment were included in the primary efficacy and safety analysis, which was defined as a modified intention-to-treat (ITT) set. Data are reported as of December 12, 2022. Descriptive statistics were used for categorical variables. PFS and OS were estimated using the Kaplan-Meier method. The median follow-up time was analyzed using the reverse Kaplan-Meier method. The logrank test was performed to compare the differences across groups. Hazard ratios (HRs) and corresponding 95% confidence interval (CI) values were estimated using the Cox proportional hazards regression model. The Fisher's exact test or χ^2 test (when appropriate) was used for comparing the proportions across groups. The Mann-Whitney U (Wilcoxon rank sum) test or t-test (when appropriate) was used to compare the means (and medians) between the 2 groups. Statistical analyses were performed using SAS version 9.4 and GraphPad Prism (version 6.00) software. Further analyses were performed in R (version 3.6.3) using the packages ComplexHeatmap (version 2.8.0), OlinkAnalyze (version 3.4.1), DESeq2 (version 1.40.1), dplyr (version 1.1.2), tidyverse (version 2.0.0), survival (version 3.5), ggplot2 (version 3.4.2), survminer (version 0.4.9), stats (version 4.3.0), ggalluvial (version 0.12.3), corrplot (version 0.92), ggcorrplot (version 0.1.4), ggpubr (version 0.6.0), and timeROC (version 0.4).

Reporting summary

Further information on research design is available in the Nature Portfolio Reporting Summary linked to this article.

Data availability

The raw ctDNA sequencing data can be accessed through the Genome Sequence Archive (GSA) under the accession code HRA005098. Sequencing data are available under restricted access due to patient privacy reasons. Access can be obtained by completing the application form via GSA-Human System or by contacting the corresponding authors. All requests for further data sharing will be reviewed by the Ethics Review Committee of Zhongshan Hospital affiliated to Fudan University, Shanghai, China to verify whether the request is subject to any intellectual property or confidentiality obligations. Requests for access to de-identified individual-level data from this trial can be submitted via email to T.L. (liu.tianshu@zs-hospital.sh.cn) with detailed proposals for approval and will be responded to within 30 days. The study protocol is available in the Supplementary Information file. The remaining data are available within the Article, Supplementary Information or Source Data file. Source data are provided with this paper.

Code availability

Custom code for data processing and analysis is available at https://doi.org/10.5281/zenodo.12798042[47].

References

1. Benson, A. B. et al. Rectal Cancer, Version 2.2022, NCCN Clinical Practice Guidelines in Oncology. *J. Natl Compr. Canc Netw.* **20**, 1139–1167 (2022).
2. Benson, A. B. et al. Colon Cancer, Version 2.2021, NCCN Clinical Practice Guidelines in Oncology. *J. Natl Compr. Canc Netw.* **19**, 329–359 (2021).
3. Grothey, A. et al. Regorafenib monotherapy for previously treated metastatic colorectal cancer (CORRECT): an international,

multicentre, randomised, placebo-controlled, phase 3 trial. *Lancet* **381**, 303–312 (2013).
4. Mayer, R. J. et al. Randomized trial of TAS-102 for refractory metastatic colorectal cancer. *N. Engl. J. Med* **372**, 1909–1919 (2015).
5. Cremolini, C. et al. Rechallenge for Patients With RAS and BRAF Wild-Type Metastatic Colorectal Cancer With Acquired Resistance to First-line Cetuximab and Irinotecan: A Phase 2 Single-Arm Clinical Trial. *JAMA Oncol.* **5**, 343–350 (2019).
6. Sartore-Bianchi, A. et al. Circulating tumor DNA to guide rechallenge with panitumumab in metastatic colorectal cancer: the phase 2 CHRONOS trial. *Nat. Med* **28**, 1612–1618 (2022).
7. Lenz, H. J. et al. First-Line Nivolumab Plus Low-Dose Ipilimumab for Microsatellite Instability-High/Mismatch Repair-Deficient Metastatic Colorectal Cancer: The Phase II CheckMate 142 Study. *J. Clin. Oncol.* **40**, 161–170 (2022).
8. Diaz, L. A. Jr et al. Pembrolizumab versus chemotherapy for microsatellite instability-high or mismatch repair-deficient metastatic colorectal cancer (KEYNOTE-177): final analysis of a randomised, open-label, phase 3 study. *Lancet Oncol.* **23**, 659–670 (2022).
9. Kawazoe, A. X. R. et al. Lenvatinib Plus Pembrolizumab Versus Standard of Care for Previously Treated Metastatic Colorectal Cancer: Final Analysis of the Randomized, Open-Label, Phase III LEAP-017 Study. *J. Clin. Oncol.* **42**, 2918–2927 (2024).
10. Eng, C. et al. Atezolizumab with or without cobimetinib versus regorafenib in previously treated metastatic colorectal cancer (IMblaze370): a multicentre, open-label, phase 3, randomised, controlled trial. *Lancet Oncol.* **20**, 849–861 (2019).
11. Pozzi, C. et al. The EGFR-specific antibody cetuximab combined with chemotherapy triggers immunogenic cell death. *Nat. Med.* **22**, 624–631 (2016).
12. Inoue, Y. et al. Cetuximab strongly enhances immune cell infiltration into liver metastatic sites in colorectal cancer. *Cancer Sci.* **108**, 455–460 (2017).
13. Woolston, A. et al. Genomic and Transcriptomic Determinants of Therapy Resistance and Immune Landscape Evolution during Anti-EGFR Treatment in Colorectal Cancer. *Cancer Cell* **36**, 35–50.e9 (2019).
14. Lee, S. C., Srivastava, R. M., Lopez-Albaitero, A., Ferrone, S. & Ferris, R. L. Natural killer (NK): dendritic cell (DC) cross talk induced by therapeutic monoclonal antibody triggers tumor antigen-specific T cell immunity. *Immunol. Res.* **50**, 248–254 (2011).
15. Taylor, R. J. et al. Ex vivo antibody-dependent cellular cytotoxicity inducibility predicts efficacy of cetuximab. *Cancer Immunol. Res* **3**, 567–574 (2015).
16. Srivastava, R. M. et al. Cetuximab-activated natural killer and dendritic cells collaborate to trigger tumor antigen-specific T-cell immunity in head and neck cancer patients. *Clin. Cancer Res.* **19**, 1858–1872 (2013).
17. Yang, X., Zhang, X., Mortenson, E. D., Radkevich-Brown, O., Wang, Y. & Fu, Y. X. Cetuximab-mediated tumor regression depends on innate and adaptive immune responses. *Mol. Ther.* **21**, 91–100 (2013).
18. Sacco, A. G. et al. Pembrolizumab plus cetuximab in patients with recurrent or metastatic head and neck squamous cell carcinoma: an open-label, multi-arm, non-randomised, multicentre, phase 2 trial. *Lancet Oncol.* **22**, 883–892 (2021).
19. Martinelli, E. et al. Cetuximab Rechallenge Plus Avelumab in Pretreated Patients With RAS Wild-type Metastatic Colorectal Cancer: The Phase 2 Single-Arm Clinical CAVE Trial. *JAMA Oncol.* **7**, 1529–1535 (2021).
20. Chung, Y. M. et al. Sensitizing tumors to anti-PD-1 therapy by promoting NK and CD8+ T cells via pharmacological activation of FOXO3. *J. Immunother. Cancer.* **9**, e002772 (2021).
21. Lee, Y. M. et al. SN-38, an active metabolite of irinotecan, enhances anti-PD-1 treatment efficacy in head and neck squamous cell carcinoma. *J. Pathol.* **259**, 428–440 (2023).
22. Heitzer, E., Haque, I. S., Roberts, C. E. S. & Speicher, M. R. Current and future perspectives of liquid biopsies in genomics-driven oncology. *Nat. Rev. Genet.* **20**, 71–88 (2019).
23. Kagawa, Y. et al. Combined Analysis of Concordance between Liquid and Tumor Tissue Biopsies for RAS Mutations in Colorectal Cancer with a Single Metastasis Site: The METABEAM Study. *Clin. Cancer Res* **27**, 2515–2522 (2021).
24. Assaf, Z. J. F. et al. A longitudinal circulating tumor DNA-based model associated with survival in metastatic non-small-cell lung cancer. *Nat. Med.* **29**, 859–868 (2023).
25. Kim, S. et al. Dynamic changes in longitudinal circulating tumour DNA profile during metastatic colorectal cancer treatment. *Br. J. Cancer* **127**, 898–907 (2022).
26. Vidal, J. et al. Liquid Biopsy Detects Early Molecular Response and Predicts Benefit to First-Line Chemotherapy plus Cetuximab in Metastatic Colorectal Cancer: PLATFORM-B Study. *Clin. Cancer Res* **29**, 379–388 (2023).
27. Lee, B. et al. Distinct Serum Immune Profiles Define the Spectrum of Acute and Chronic Pancreatitis From the Multicenter Prospective Evaluation of Chronic Pancreatitis for Epidemiologic and Translational Studies (PROCEED) Study. *Gastroenterology.* **165**, 173–186 (2023).
28. Tang, Z. et al. Multiplex immune profiling reveals the role of serum immune proteomics in predicting response to preoperative chemotherapy of gastric cancer. *Cell Rep. Med.* **4**, 100931 (2023).
29. Leibovitzh, H. et al. Immune response and barrier dysfunction-related proteomic signatures in preclinical phase of Crohn's disease highlight earliest events of pathogenesis. *Gut.* **72**, 1462–1471 (2023).
30. Li, J. et al. Effect of Fruquintinib vs Placebo on Overall Survival in Patients With Previously Treated Metastatic Colorectal Cancer: The FRESCO Randomized Clinical Trial. *JAMA* **319**, 2486–2496 (2018).
31. Cunningham, D. et al. Cetuximab monotherapy and cetuximab plus irinotecan in irinotecan-refractory metastatic colorectal cancer. *N. Engl. J. Med.* **351**, 337–345 (2004).
32. Masuishi, T. et al. Phase 2 study of irinotecan plus cetuximab rechallenge as third-line treatment in KRAS wild-type metastatic colorectal cancer: JACCRO CC-08. *Br. J. Cancer* **123**, 1490–1495 (2020).
33. Tsuji, A. et al. Phase II Study of Third-Line Panitumumab Rechallenge in Patients with Metastatic Wild-Type KRAS Colorectal Cancer Who Obtained Clinical Benefit from First-Line Panitumumab-Based Chemotherapy: JACCRO CC-09. *Target Oncol.* **16**, 753–760 (2021).
34. Fountzilas, C. et al. Phase Ib/II Study of Cetuximab plus Pembrolizumab in Patients with Advanced RAS Wild-Type Colorectal Cancer. *Clin. Cancer Res* **27**, 6726–6736 (2021).
35. Quan, M. et al. China special issue on gastrointestinal tumors-Cetuximab retreatment plus camrelizumab and liposomal irinotecan in patients with RAS wild-type metastatic colorectal cancer: Cohort B of the phase II CRACK study. *Int J. Cancer* **153**, 1877–1884 (2023).
36. Fukuoka, S. et al. Regorafenib Plus Nivolumab in Patients With Advanced Gastric or Colorectal Cancer: An Open-Label, Dose-Escalation, and Dose-Expansion Phase Ib Trial (REGONIVO, EPOC1603). *J. Clin. Oncol.* **38**, 2053–2061 (2020).
37. Andrea, J. et al. Botensilimab plus balstilimab in relapsed/refractory microsatellite stable metastatic colorectal cancer: a phase 1 trial. *Nat Med.* https://doi.org/10.1038/s41591-024-03083-7 (2024).
38. Fakih, M. et al. Regorafenib, Ipilimumab, and Nivolumab for Patients With Microsatellite Stable Colorectal Cancer and Disease Progression With Prior Chemotherapy: A Phase 1 Nonrandomized Clinical Trial. *JAMA Oncol.* **9**, 627–634 (2023).
39. Wang, F. et al. Regorafenib plus toripalimab in patients with metastatic colorectal cancer: a phase Ib/II clinical trial and gut microbiome analysis. *Cell Rep. Med.* **2**, 100383 (2021).

40. Cousin, S. et al. REGOMUNE: A phase II study of regorafenib plus avelumab in solid tumors-Results of the non-MSI-H metastatic colorectal cancer (mCRC) cohort. *J. Clin. Oncol.* **38**, 2 (2020).
41. Zhang, Q. et al. Prognostic and Predictive Impact of Circulating Tumor DNA in Patients with Advanced Cancers Treated with Immune Checkpoint Blockade. *Cancer Discov.* **10**, 1842–1853 (2020).
42. Nabet, B. Y. et al. Noninvasive Early Identification of Therapeutic Benefit from Immune Checkpoint Inhibition. *Cell* **183**, 363–76.e13 (2020).
43. Rozeman, E. A. et al. Survival and biomarker analyses from the OpACIN-neo and OpACIN neoadjuvant immunotherapy trials in stage III melanoma. *Nat. Med.* **27**, 256–263 (2021).
44. Assarsson, E. et al. Homogenous 96-plex PEA immunoassay exhibiting high sensitivity, specificity, and excellent scalability. *PLoS One* **9**, e95192 (2014).
45. Lundberg, M., Eriksson, A., Tran, B., Assarsson, E. & Fredriksson, S. Homogeneous antibody-based proximity extension assays provide sensitive and specific detection of low-abundant proteins in human blood. *Nucleic Acids Res.* **39**, e102 (2011).
46. Garg, M. et al. Tumour gene expression signature in primary melanoma predicts long-term outcomes. *Nat. Commun.* **12**, 1137 (2021).
47. Xiaojing Xu, LA, et al. Tislelizumab Plus Cetuximab and Irinotecan in Patients with Refractory MSS and RAS Wild-Type Metastatic Colorectal Cancer: Clinical Benefit and Longitudinal Genoproteomic Analysis. https://github.com/corefacilitygenecast/CRC-code/, https://doi.org/10.5281/zenodo.12798042 (2024).

Acknowledgements

We thank the patients, their families, and caregivers for participating in the study, BeiGene Ltd. for free tislelizumab support, and Genecast Biotechnology Co., Ltd. for NGS and Olink analysis. They did not participate in study design, clinical data collection and analysis or manuscript writing. The work was supported by the National Nature Science Foundation of China [82373402 (T.L.), 82172925 (T.L.), 82272775 (L.A.)], Clinical Research Foundation of Zhongshan Hospital Affiliated to Fudan University (2020ZSLC02, T.L.), Funding from Science and Technology Commission of Shanghai Municipality (19DZ1910102, T.L.), Shanghai ShenKang Research Physicians Innovation and Transformation Ability Training Project (SHDC2022CRT001, T.L.), Shanghai Rising-Star Program (21QA1401600, L.A.) and Outstanding Youth of Zhongshan Hospital Affiliated to Fudan University (2021ZSYQ01, L.A.).

Author contributions

X.X., L.A., K.H., L.L., and M.L. contributed equally to this work. X.X., L.A., L.L., M.L., Y.Yu., and T.L. conceived and designed the study. X.X., L.L., Y.W., Y.C., W.L., Q.Li., S.Y., Y.F., Q.Liu., Y.Yu., and T.L. provided study material or treated patients. All authors collected and assembled the data. X.X., L.A., K.H., M.L., Y.Yang., J.Z., and F.X. performed all the bioinformatic analyses and developed the tables and figures. X.X., L.A., and K.H. conducted the literature search and wrote the manuscript. All authors were involved in the critical review of the manuscript and approved the final version.

Competing interests

The authors declare no competing interests.

Additional information

Supplementary information The online version contains supplementary material available at https://doi.org/10.1038/s41467-024-51536-x.

Correspondence and requests for materials should be addressed to Yiyi Yu or Tianshu Liu.

Peer review information *Nature Communications* thanks Matthew Reilley, Vivien Yin and the other, anonymous, reviewer(s) for their contribution to the peer review of this work. A peer review file is available.